Gerzaguet *et al. EURASIP Journal on Wireless Communications and Networking* (2017) 2017:13
DOI 10.1186/s13638-016-0792-0

EURASIP Journal on Wireless Communications and Networking

RESEARCH Open Access

The 5G candidate waveform race: a comparison of complexity and performance

Robin Gerzaguet[1*], Nikolaos Bartzoudis[2], Leonardo Gomes Baltar[3], Vincent Berg[1], Jean-Baptiste Doré[1], Dimitri Kténas[1], Oriol Font-Bach[2], Xavier Mestre[2], Miquel Payaró[2], Michael Färber[3] and Kilian Roth[3]

Abstract

5G will have to cope with a high degree of heterogeneity in terms of services and requirements. Among these latter, the flexible and efficient use of non-contiguous unused spectrum for different network deployment scenarios is considered a key challenge for 5G systems. To maximize spectrum efficiency, the 5G air interface technology will also need to be flexible and capable of mapping various services to the best suitable combinations of frequency and radio resources. In this work, we propose a comparison of several 5G waveform candidates (OFDM, UFMC, FBMC and GFDM) under a common framework. We assess spectral efficiency, power spectral density, peak-to-average power ratio and robustness to asynchronous multi-user uplink transmission. Moreover, we evaluate and compare the complexity of the different waveforms. In addition to the complexity analysis, in this work, we also demonstrate the suitability of FBMC for specific 5G use cases via two experimental implementations. The benefits of these new waveforms for the foreseen 5G use cases are clearly highlighted on representative criteria and experiments.

Keywords: 5G, Waveform, OFDM, GFDM, UFMC, FBMC

1 Introduction

The Next Generation Mobile Networks (NGMN) Alliance highlights in [1] the necessity to make more spectrum available in the existing sub-6 GHz radio bands and introduce new agile waveforms that exploit the existing underutilized fragmented spectrum, in order to satisfy specific fifth-generation (5G) operating scenarios. The goal of the waveform symbiosis will therefore be to flexibly optimize the use of existing underutilized spectrum resources, guarantee interference-free coexistence with legacy transmissions and provide an improved spectral containment compared to the orthogonal frequency division multiplexing (OFDM) modulation that is widely used in broadband wireless systems operating below 6 GHz. The need for a new 5G waveform has also been discussed in the context of asynchronous multi-user 5G operating scenarios [2], which envision sporadic access of mobile nodes that rapidly enter in a dormant state after a data transaction. This feature, called fast dormancy, has been identified as the root cause of significant signaling overhead on cellular networks [3]. Relaxed synchronization schemes have been considered to limit the amount of required signaling. This is the case, for instance, when the mobile node carries only a coarse knowledge of time synchronization. The massive number of devices and the support of multi-point transmissions in 5G use cases will imply the use of relaxed synchronization, potentially leading to strong inter-user interference.

OFDM is a multicarrier communication scheme that has been widely adopted in a number of different wired and wireless communication systems. Among others, 3GPP adopted it as the underlying physical layer (PHY) technology in mobile broadband systems denoted as 4G long-term evolution (LTE). It exhibits some intrinsic drawbacks including frequency leakage caused by its rectangular pulse shape, spectral efficiency loss due to the use of a cyclic prefix (CP) and need for fine time and frequency synchronization in order to preserve the carrier orthogonality, which guarantees a low level of intra and inter-cell interferences. To overcome these limitations, several alternative candidates have been intensively studied in the literature over the past few years, such as universal filtered multi carrier (UFMC) [2], generalized

*Correspondence: robin.gerzaguet@cea.fr
[1]CEA-Leti, Minatec Campus, Grenoble, France
Full list of author information is available at the end of the article

frequency division multiplexing (GFDM) [4] and filter bank multicarrier (FBMC) [5].

This paper presents these popular candidate 5G waveforms and compares them in terms of specific performance features such as spectral efficiency, power spectral density and peak-to-average power ratio (PAPR). In addition, we also analyze multi-user interference scenarios and compare the performance of candidate waveforms for several delays and carrier frequency offsets, accounting for a different number of guard carriers and according to different waveform parameters. We also compare their baseband computational complexity using as a baseline reference the current waveforms used in 4G LTE downlink (DL) and uplink (UL). Finally, we present practical implementations of FBMC-based waveforms demonstrating the feasibility of adopting such PHY-layer schemes and verifying their superior performance when compared to CP-OFDM, under shared licensed spectrum use cases (i.e. a driving technology of several 5G use cases).

The 3GPP is in the process of studying and eventually adopting proposals for the new 5G air interface, which eventually will be standardized within 2017. Depending on the end use and specific operation band (i.e. sub 6 GHz and millimeter wave frequencies), it is expected that two versions of 5G radio access waveforms will be standardized. Previous works from other researchers have focused either on a specific 5G candidate waveform [6, 7] or on comparing different performance features (or target applications) [8, 9] from the ones presented in this paper. Details related to real-time implementation of 5G waveforms [10] and laboratory-based experimental validation [11, 12] are very scarce in the literature and typically provide benchmarking of a particular use case [13]. The work presented in this paper is in this sense more transversal covering key performance aspects of the most popular 5G waveform candidates, along with a computational complexity analysis and practical real-time implementations targeting field programmable gate array (FPGA) devices under realistic spectrum cohabitation scenarios (including experimental validation). Other sources related to the work presented in this paper are encountered in white papers [14] or application notes [15] describing add-on software libraries that target arbitrary waveform generation instruments. Such software pre-products are used to underpin the market readiness of the instrumentation and measurements sector and its ability to timely provide test solutions once the 5G air interface will be finally standardized; typically, the non-academic references do not enter in a fine-grain analysis of the computational complexity and do not present hardware implementation details of the different candidate 5G waveforms.

The main objectives of this paper, in addition to be a comprehensive introduction and comparison of the most promising multicarrier waveforms are to (i) provide a unified comparison framework where waveform performance are assessed wrt representative criteria, (ii) perform a baseband complexity analysis of these aforementioned waveforms and (iii) propose implementation examples for FBMC as well as to describe a use case example where FBMC shows its interest. This proposed analysis shows the interest in designing, studying and implementing alternatives to classic CP-OFDM.

This paper is organized as follows: the main 5G waveforms candidates are presented in Section 2. A comparison regarding several criteria (spectral density, power spectral density, PAPR and robustness in asynchronous multi-user scenario) and a complexity analysis are described in Section 3. Two practical implementations of FBMC are presented in Section 4. Finally, the last section draws some conclusions.

2 5G candidate waveforms background

In this section, we briefly introduce the main 5G waveform candidates that we will compare and study in Sections 3 and 4.

2.1 CP-OFDM

In CP-OFDM, a block of complex symbols is mapped onto a set of orthogonal carriers (see Fig. 1). Due to the use of inverse fast Fourier transform (IFFT) (resp. FFT) process of size N_{FFT}, CP-OFDM architecture has a low complexity. The principle of OFDM is to divide the total bandwidth into N_{FFT} carriers, so that channel equalization can often be reduced as a one tap coefficient per carrier. Finally, a cyclic prefix (CP) is inserted. It guarantees circularity of the OFDM symbol, if the delay spread of the multipath channel is lower than the CP length. It, however, leads to a loss of spectral efficiency, as the CP is used to transmit redundant data. To limit the PAPR, an additional discrete Fourier transform (DFT) (resp. IDFT) a precoding stage can be inserted before the IFFT (resp. after FFT), leading to the so-called single carrier frequency division multiple access (SC-FDMA) used in the uplink of 3GPP-LTE.

2.2 FBMC

FBMC waveform consists in a set of parallel data that are transmitted through a bank of modulated filters. The prototype filter, parametrized by the overlapping factor K, can be chosen to have very low adjacent channel leakage. One may differentiate between two main variants of FBMC: one based on complex (QAM) signaling, also referred to as filtered multi tone (FMT), and another based on real valued offset QAM (OQAM) symbols, also referred to as FBMC/OQAM. The latter ensure orthogonality in real domain to maximize spectral efficiency. The first variant (FMT) is currently employed in standards

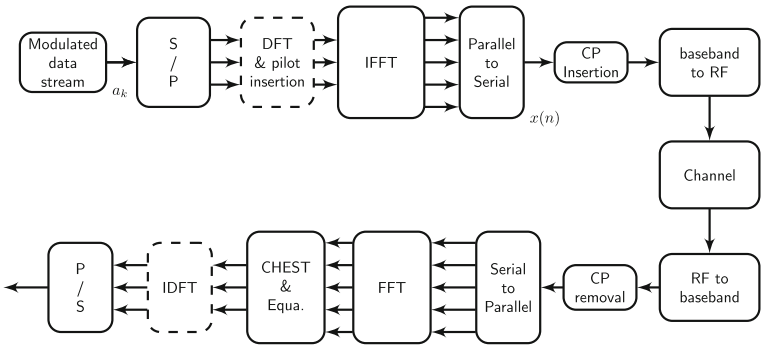

Fig. 1 CP-OFDM transceiver (additional SC-FDMA stages in dash). S/P and P/S, respectively, denote parallel to serial and serial to parallel

like Telecommunication Equipment Distribution Service (TEDS), and achieves orthogonality among subcarriers by physically reducing their frequency domain overlapping, thus reducing the SE in a similar proportion as CP-OFDM.

FBMC/OQAM, on the contrary, is able to achieve the maximum SE [16] by imposing the orthogonality in the real domain only. Given the SE optimality of FBMC/OQAM, this variant is universally considered as the baseline FBMC modulation. Multiple alternative ways of implementing FBMC-OQAM in a computationally efficient manner are existing, although the most important are polyphase networks (PPN) and frequency spreading (FS) implementations. In PPN architecture (see Fig. 2), OQAM symbols feed an FFT of size N_{FFT} and then into a PPN. The receiver applies matched filtering before a FFT of size N_{FFT} and multi-tap equalization is performed in a per carrier basis [17].

In FS-FBMC (see Fig. 3), OQAM symbols are filtered in frequency domain [5]. The result then feeds an IFFT of size KN_{FFT}, followed by an overlap and sum operation. At the receiver side, a sliding window selects KN_{FFT} points every $N_{\text{FFT}}/2$ samples [18]. A FFT of size KN_{FFT} is applied followed by filtering by the prototype matched filter.

2.3 UFMC

UFMC waveform is a derivative of OFDM waveform combined with post-filtering, where a group of carriers is filtered by using a frequency domain efficient implementation [2]. This subband filtering operation is motivated by the fact that the smallest unit used by the scheduling algorithm in frequency domain in 3GPP LTE is a resource block (RB), which is a group of 12 carriers. The filtering operation leads to a lower out-of-band leakage than for OFDM. The UFMC transmitter (see Fig. 4) is composed of B subband filtering that modulate the B data blocks. The transmitted signal uses no CP, but there is still a spectral efficiency loss due to the time transient (tails) of the shaping filter. The Rx stage is composed of a $2N_{\text{FFT}}$ point FFT, which is then decimated by a factor 2 to recover the data. A windowing stage can also be inserted before the FFT. It introduces interference between carriers but is interesting to consider for asynchronous uplink transmissions as it helps to separate contiguous users.

2.4 GFDM

GFDM waveform is based on the time-frequency filtering of a data block, which leads to a flexible, non-orthogonal waveform [4]. A data block is composed of K carriers and

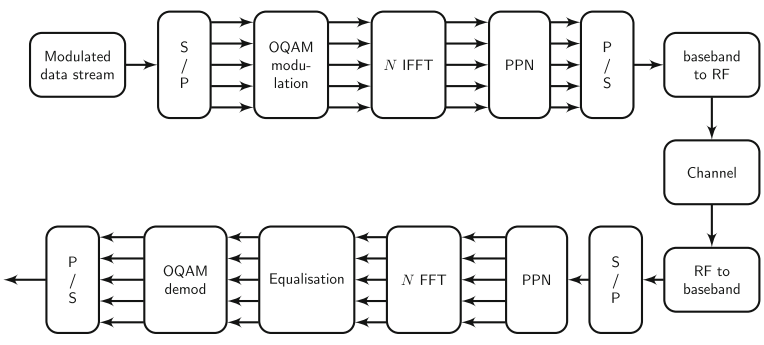

Fig. 2 PPN-FBMC transceiver

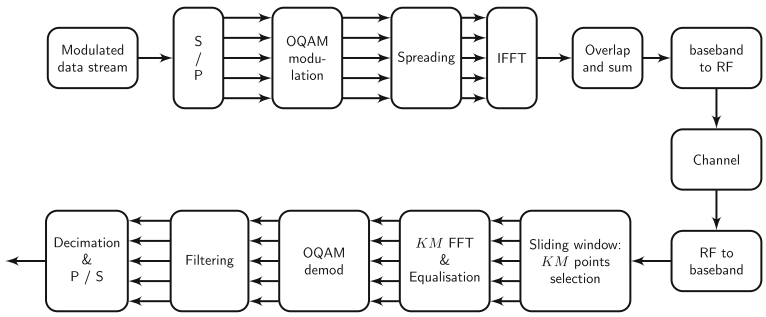

Fig. 3 FS-FBMC transceiver

M time slots, and transmits $N = KM$ complex modulated data. In this paper, we consider that the data is cyclic filtered by a root-raised-cosine (RRC) filter that is translated into both frequency and time domains (see Fig. 5) as it is customarily done [4, 6]. To avoid inter-symbol interference, a CP is added at the end of each block of symbols. To further improve the spectral location, a windowing process can be added in the transmitter.

Several receiver architectures have been investigated in the literature for GFDM, and we consider in this paper a matched filter (MF) receiver scheme: each received block is filtered by the same time and frequency translated filters as in the transmission stage [4]. As the modulation is non-orthogonal, it is necessary to implement an interference cancellation (IC) scheme [19], which improves the performance but severely increases the complexity of the receiver. More recently, OQAM was also considered in GFDM to allow the use of less complex linear receivers instead of IC [20].

3 Performance comparison and complexity

In Section 2, 5G candidate waveforms have been introduced, and their main parameters and architectures have been described. In this section, we compare the waveforms regarding several criteria: their power spectral density, their spectral efficiency and their PAPR. Besides, a performance comparison of the waveform candidates in a typical multi-user asynchronous access scheme is done. We eventually compare the computational complexity of the different waveforms.

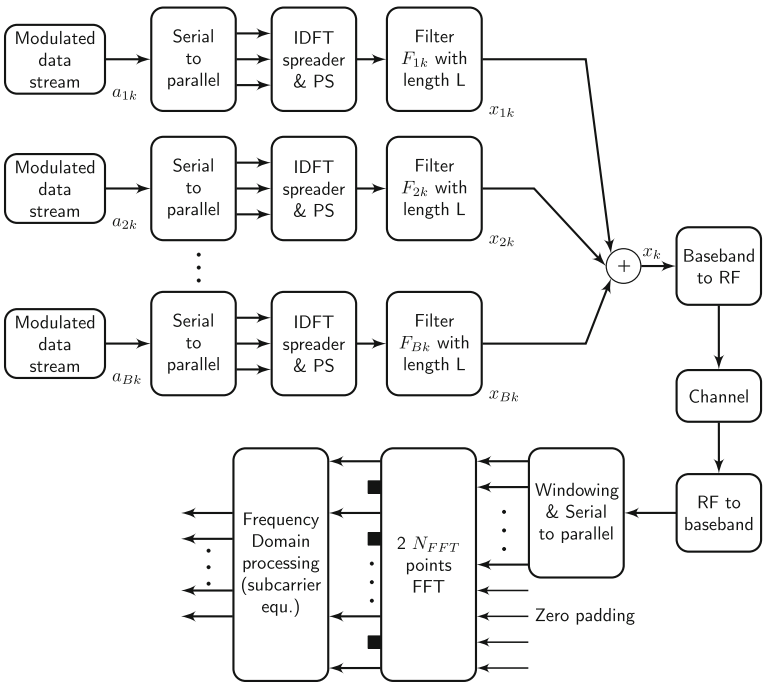

Fig. 4 UFMC transceiver

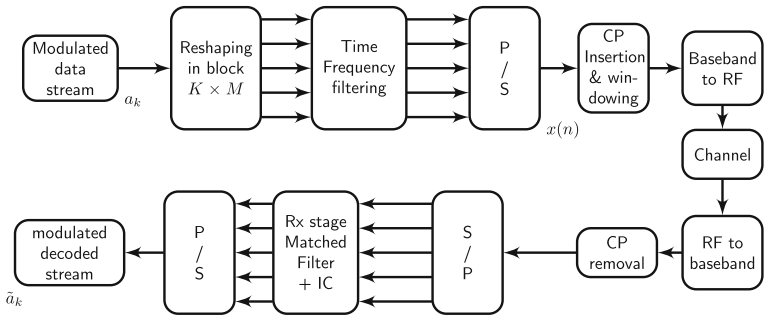

Fig. 5 GFDM transceiver

3.1 Spectral efficiency, power spectral density and PAPR comparison

We consider the parameters based on LTE 10 MHz with QPSK modulation, a FFT size of 1024 (and a CP size of 72 samples) and a sampling frequency of 15.36 MHz. For FBMC-OQAM, the overlapping factor is set to 4 using the PHYDYAS filter [16]. For GFDM, the number of symbols per carrier M is set to 15, and the roll-off factor of the RRC filter is set to 0.1. For UFMC, we use a Dolph-Chebyshev filter of length $L = 73$ (with 40 dB attenuation) to have the same SE as OFDM [2]. In the following, we compare the SE (Fig. 6), the power spectral density (Fig. 7), and the complementary cumulative distribution function (CCDF) of the PAPR (Fig. 8) of selected 5G candidate waveforms, which constitute a representative set of performance metrics.

We first consider the spectral efficiency on Fig. 6. In OFDM, SC-FDMA, GFDM and UFMC, the spectral efficiency does not depend on the burst duration and it is a function of the modulation parameters. But for FBMC-OQAM, it depends on the frame duration, and the spectral efficiency loss is due to the transient state of the shaping filter if assumed that no transmission takes place during this period. Thus, there is no constant loss per symbol and the spectral efficiency increases with the burst duration to reach an asymptotic level equal to the modulation order. For GFDM, the spectral efficiency is higher compared to OFDM as a GFDM symbol is M times longer compared to an OFDM one. Indeed, for GFDM, the spectral efficiency loss due to the CP insertion is limited as there is one CP per GFDM symbol (i.e. 1 CP per M equivalent OFDM symbols).

We now consider the power spectral density in Fig. 7. To better stress the impact of the adjacent channel leakage, we consider two users that occupy 36 carriers (3 RBs), with 12 guard carriers (1 RB) as guard band. The best spectral localization is obtained with FBMC-OQAM. GFDM has a slightly lower out-of-band leakage compared to OFDM but is clearly outperformed by UFMC. With the addition of the windowing process, GFDM becomes comparable to the UFMC.

We compute on Fig. 8 the CCDF of the PAPR for the considered waveforms, for a burst duration of 3 ms. SC-FDMA, due to its (quasi) single carrier property, offers the best performance. The other modulations, which are multicarrier, have a higher PAPR and none of the multicarrier

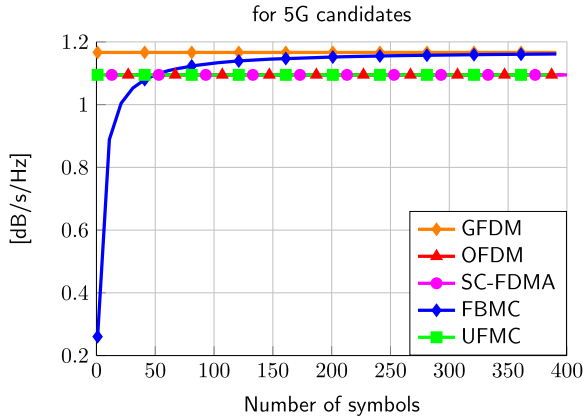

Fig. 6 Spectral efficiency vs burst duration for QPSK

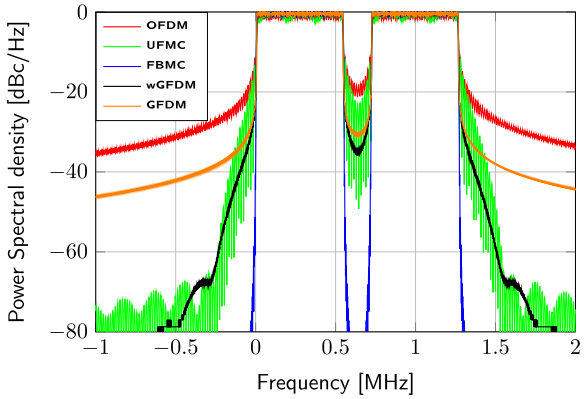

Fig. 7 Power spectral density of the waveforms

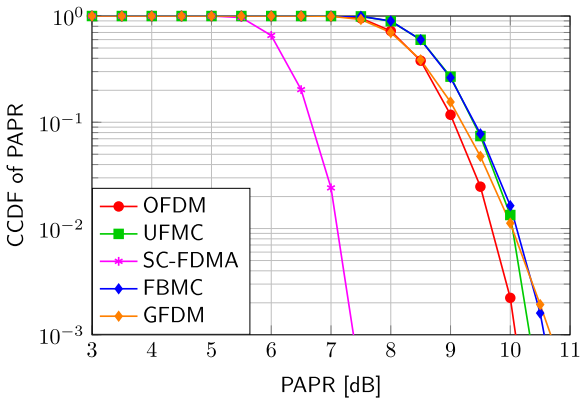

Fig. 8 CCDF of PAPR

candidates with the chosen parametrization offers better performance than OFDM. However, it should also be noted that the gap is small, around 0.5 dB.

3.2 Multi-user access scheme

In this section, we compare the performance of the 5G waveform candidates in a typical multi-user asynchronous access scheme [21]. We consider two users, user equipment (UE) 1 and UE 2. The first user occupies three RBs and is assumed to be perfectly synchronized in time and frequency domains with its serving base station. The secondary user occupies nine RBs and suffers from a delay error (i.e. a timing offset) and a potential carrier frequency offset due to a synchronization mismatch with downlink channel. Due to the timing and frequency errors, the secondary user interferes with the first one. The data stream of the first user is decoded (assuming no channel and no noise), and the performance in terms of mean square error (MSE) on the decoded constellation is evaluated. The interference only comes from the interferer user. The spacing in terms of guard carriers between the two users is variable: no guard carrier (contiguous allocation), one guard carrier and two guard carriers.

We consider the previously introduced waveforms. OFDM and SC-FDMA have the same performance, so only OFDM curves are plotted. For GFDM and UFMC, we consider the impact of additional windowing (denoted, respectively, by wGFDM and wUFMC). The performance results are depicted on Fig. 9, on the left without carrier frequency offset and on the right with a carrier frequency offset of 10%.

We have shown in Fig. 7 that windowing for GFDM lowers the out-of-band leakages, as it improves the spectral isolation between users. For the multi-user scenario, it is shown that the performance without windowing is better in case of low delay error value (as the interference introduced by the windowing effect is not negligible), but that the performance with windowing is better when the delay error does not belong to the CP interval. This is due to the trade-off between the self-interference introduced by the windowing and the isolation gain between users offered by the windowing.

The windowing effect for UFMC is different from GFDM as the windowing is applied on the receiver side, and has no consequences on the power spectral density of the transmitted signal. It however improves the performance in the multi-user scenario. These results are very similar to the results presented in [2] and validate the positive impact of the windowing scheme for UFMC. Due to the very good spectral location of the FBMC prototype filter, the MSE reaches its lower bound as soon as a guard carrier is inserted. Besides that, the performance is independent from the delay error value.

We now consider the performance with an additional carrier frequency offset of 10%. Due to the additional interference introduced by the frequency error, the MSE is higher for all the waveforms, except for FBMC-OQAM with at least one guard carrier. For OFDM, the orthogonality cannot be preserved anymore and a strong interference level is present even if the delay error belongs to the CP interval. Besides that, without guard band, the performance of GFDM and FBMC-OQAM becomes very similar, and is slightly better than UFMC out of CP. If the guard carrier number is non-null, FBMC exhibits no interference, and the hierarchy between the other candidates is the same as without carrier frequency offset.

As a conclusion, GFDM, UFMC and FBMC-OQAM are promising candidates for the multi-user asynchronous access scheme and outperform classic CP-OFDM. UFMC waveform is an interesting option as the SE is comparable to OFDM and the pulse shaping function gives robustness to asynchronous access. Backward compatibility with well-known OFDM algorithms (e.g. channel estimation, massive-input massive-output (MIMO) detectors) is also preserved. FBMC and GFDM go further since the well-localized frequency response enables the use of fragmented spectrum with minor interference on adjacent bands. Very good performances are demonstrated in non-synchronous access as well. However, transceiver complexity should be managed and some concepts should be revisited (e.g. MIMO schemes, short packet adaptation) for a future deployment.

4 Computational complexity comparison

In this section, we perform a comparison of the computational complexity for the different waveform schemes in a single antenna configuration. We quantify the complexity in terms of the total number of real multiplications per symbol. We consider the signal processing

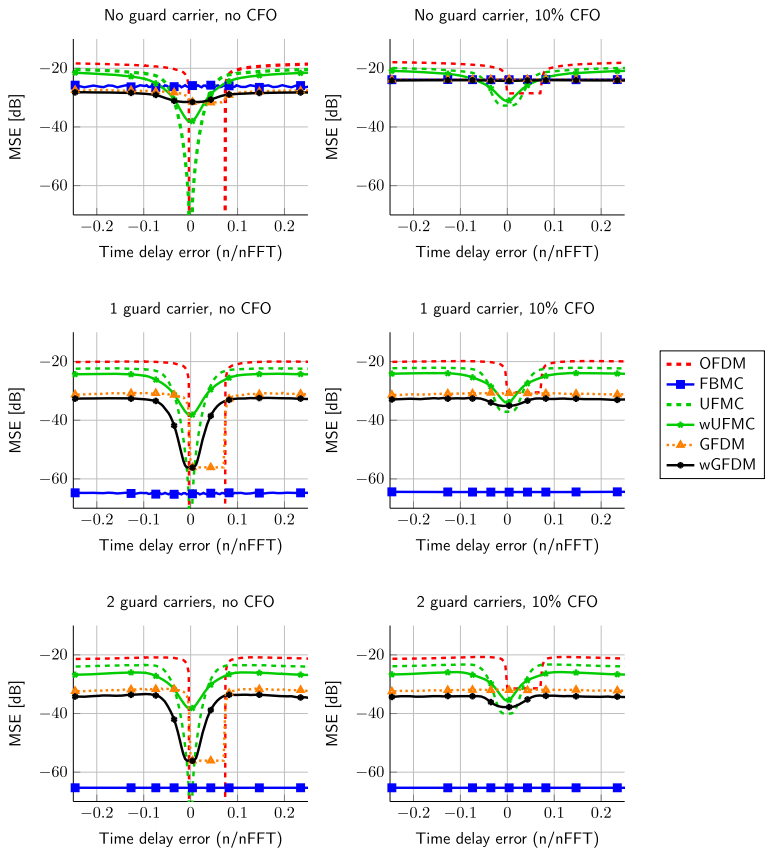

Fig. 9 Performance of the different candidate 5G waveforms in asynchronous multi-user scenario

operations involved in the generation of the MC and single-carrier (SC) signals, as well as the recovery of the subcarrier/subchannel signals and equalization in the presence of multipath propagation. Here, we do not consider the operations involved in channel estimation or calculation of the equalizer coefficients. The first reason is because those signal processing tasks are not in the user data chain, which is the one that concentrates the processing burden, and the second is because of the many existing algorithms for those tasks making the choice of one not trivial. Moreover, we assume that all systems are perfectly synchronized.

4.1 Cyclic prefix OFDM

We assume that the total of M subcarriers are available out of which M_f are occupied with symbols. We will consider first the number of real valued multiplications to transmit one block of M_f symbols. Starting with the fast Fourier transform (FFT), the number of real multiplications of a M-point FFT/ inverse FFT (IFFT) using a split-radix algorithm is given by

$$C_{\text{FFT}}(M) = M\left(\log_2(M) - 3\right) + 4. \tag{1}$$

Since the transmitter (Tx) of a CP-OFDM system is basic built with one single IFFT and by including the windowing operation we get

$$C_{\text{OFDM}}^{\text{Tx}} = C_{\text{FFT}}(M) + 4(M + L_{\text{CP}}). \tag{2}$$

For the demodulation and recovery of the subcarrier signals, two processing tasks are necessary: FFT and single-tap equalization per subcarrier. The complexity is given by

$$C_{\text{OFDM}}^{\text{Rx}} = C_{\text{FFT}}(M) + 4M_f, \tag{3}$$

for the MC demodulation and equalization.

4.2 FBMC-OQAM

Assuming an FBMC-OQAM system where the prototype filter has length KM, two approaches can be adopted for the generation and recovery of the MC signal: the polyphase-based and the frequency spread-based structures. We consider first the complexity of FBMC-OQAM implemented with a structure based on the polyphase decomposition of the prototype filter and using a direct form realization of the polyphase components (PC) [22]. The Tx is composed of three steps after the OQAM modulation:

- Phase rotations to get linear phase filters in each subcarrier
- IFFT
- Polyphase filtering followed by block overlapping of 50%

At the Rx side, similar operations in the inverted order are implemented including one more step: polyphase filtering, FFT, multitap channel equalization per sub-carrier with an equalizer of length L_{eq} and the OQAM demodulation. The phase rotations at the receiver side can be embedded in the equalizer coefficients. The total number of real valued multiplications is then given by

$$C^{\text{Tx}}_{\text{PC-FB}} = 2C_{\text{FFT}}(M) + 4MK + 4M_f, \quad (4)$$
$$C^{\text{Rx}}_{\text{PC-FB}} = 2C_{\text{FFT}}(M) + 4MK + 4L_{\text{eq}}M_f, \quad (5)$$

where we have taken into account that the IFFT and the polyphase network work with double of the QAM symbol rate and that the coefficients of the prototype are real valued.

The second approach is a frequency domain filtering, a.k.a. frequency spread [23] based FBMC, featuring also a general prototype with length KM and designed using the frequency sampling approach with only $2(K-1)$ non-zero coefficients. In this case, the structure changes drastically. The subcarrier signals have to be spread over $K+1$ frequency domain samples and each of them multiplied by one of the prototype frequency domain coefficients. The overlapping parts in frequency domain are all added and then transformed with the IFFT of size KM and finally an overlap and add of dimension $M/2$ is performed to generate the time domain signal. At the Rx side, the inverse operations are done resulting in the following complexity

$$C^{\text{Tx}}_{\text{FS-FB}} = 2C_{\text{FFT}}(KM) + 8M_f(K-1). \quad (6)$$
$$C^{\text{Rx}}_{\text{FS-FB}} = 2C_{\text{FFT}}(KM) + 16M_f(K-1), \quad (7)$$

where we have taken into account that the equalizer coefficients can be incorporated in the frequency domain coefficients of the filters.

4.3 UFMC/UF-OFDM/filtered CP-OFDM

The UFMC system can be parametrized between two extremes: in one end, one single CP-OFDM signal is filtered by one filter to reduce the out-of-band radiation. At the other end, each or a minimum number of resource blocks is transformed with the IFFT and filtered with its own filter. In an UFMC system with maximum granularity, B resource blocks each with M_B subcarriers require B FFTs of size M_{NB}, where each of them has only M_B non-zero inputs. The modulation is performed in the following steps: First, the signal of each subband is spread over the whole symbol length and transformed into the frequency domain. Then, the filtering is performed in the frequency domain and the sum of all subbands is converted into the time domain [24].

Instead of filtering and then transforming, a non-matched filtering is applied in the frequency domain [25]. The Rx has then three steps:

- Windowing in the time domain
- FFT transformation of size $2M$ with zero padding and half of the outputs thrown away
- Frequency domain filtering and equalization

The total number of multiplications is then given by

$$C^{\text{Tx}}_{\text{UFMC}} = B\left[C_{\text{FFT}}(2M_{\text{NB}}) + C_{\text{FFT}}(M_{\text{NB}}) + 8M_{\text{NB}}\right] + C_{\text{FFT}}(2M), \quad (8)$$
$$C^{\text{Rx}}_{\text{UFMC}} = C_{\text{FFT}}(2M) + 8M + 4M_f. \quad (9)$$

4.4 Generalized frequency division multiplexing

The generalized frequency division multiplexing (GFDM) modulation scheme is based on circular convolving each subcarrier in a block of data with a filter kernel. In contrast to OFDM, a cyclic prefix is added per block and not per symbol [6, 26]. Since a circular convolution can be calculated as a multiplication of two vectors in frequency domain, the transmitter and receiver can be efficiently implemented using the FFT. Out of a total number of subcarriers M, only M_f are used. N symbols per subcarrier are combined to form one transmission block. In total, NM_f data symbols can be transmitted per block. The prototype filter is designed to overlap with M_a adjacent subcarriers and it is typically chosen to be an RRC filter $M_a = 2$. As described in [6], excluding the trivial operations like reordering, the following signal processing tasks need to be performed at the transceiver:

- Transformation of the data signal of each subcarrier into the frequency domain
- Filtering in the frequency domain
- Transformation of the signal into the time domain

The complexity at Tx is given by

$$C^{\text{Tx}}_{\text{GFDM}} = M_f C_{\text{FFT}}(N) + 4M_f M_a N + C_{\text{FFT}}(NM). \quad (10)$$

The details of the corresponding receiver are described in [26]. It is important to mention that since the subcarriers are overlapping, it is necessary to cancel this interference to achieve a sufficient performance. In [26], the authors use the detected symbols to subtract the interference to adjacent subcarriers in an iterative fashion. For a constellation as large as 64QAM it was shown that $J = 8$ iterations are sufficient. The receiver can be divided into the following signal processing tasks:

- Transformation of the signal into the frequency domain
- Channel equalization
- Filtering in the frequency domain
- Iterative interference cancellation

The complexity at the receiver (Rx) is then given by

$$C_{\text{GFDM}}^{\text{Rx}} = C_{\text{FFT}}(NM) + 4(M_f + 2(M_a - 1))N + 4M_f M_a N + JM_f\left(2C_{\text{FFT}}(N) + 4N\right). \quad (11)$$

4.5 Numerical evaluation

In this section, we perform a comparison of the computational complexity for the different waveform schemes in a single antenna configuration. We quantify the complexity in terms of the total number of real multiplications per symbol. We consider the signal processing operations involved in the generation of the MC and SC signals, as well as the recovery of the subcarrier/subchannel signals and equalization in the presence of multipath propagation. Here, we do not consider the operations involved in channel estimation or calculation of the equalizer coefficients. The first reason is because those signal processing tasks are not in the user data chain, which is the one that concentrates the processing burden, and the second is because of the many existing algorithms for those tasks making the choice of one not trivial. Moreover, we assume that all systems are perfectly synchronized.

For the numerical evaluation, we evaluate the complexity in the base and mobile stations (BS, MS) separately and consider the number of multiplications and additions normalized by the number of transmitted QAM symbols. We assume a similar overhead in terms of training or reference signals for all waveforms. Moreover, we consider the following four scenarios:

1. Downlink with narrowband allocation per mobile station
2. Downlink with broadband allocation
3. Uplink with narrowband allocation per mobile station
4. Uplink with broadband allocation

In Scenarios 1 and 3, for each MS, six resource blocks are allocated and 17 mobiles are served simultaneously. In Scenarios 2 and 4, only one MS is served and all 1320 available frequency bins are allocated to it. The parameters are described in Table 1.

In Figs. 10 and 11, we have the complexity results for the different waveforms in different scenarios in the BS and MS.

For UFMC, we have used the most efficient structure to the best of our knowledge and the filter impulse response is set in order to get the same overhead as in CP-OFDM. For GFDM, we consider four symbols per carrier and an IC receiver with eight iterations.

Table 1 Simulation parameters

CP-OFDM	
Number of subcarriers M	2048
Number of active subcarriers M_f	1224 or 1320
CP length	144
Number of RBs B (min, max)	(6, 110)
FBMC	
Overlapping factor K	4
Number of equalizer taps/subcarrier L_{eq} (PPN)	3
UFMC	
Number of subcarriers/RB	12
Filter length	145
Size of NB FFT M_{NB}	64
GFDM	
Number of symbols/subcarrier N	4
Number of overlap subcarriers M_a	2
Number of SIC iterations J	8

We can see that PPN FBMC and GFDM involve less than three times the number of operations than SC-FDMA, while FS-FBMC involves seven times more operations and UFMC more than nine times. It should besides be noted that, in case of FBMC, UFMC and GFDM, a filtering process is embedded in the waveform generation stage. One can note that if an agile access to fragmented spectrum is needed, a filtering process should be added to OFDM transmitter (with the granularity of a RB) and then the complexity of OFDM-based waveform increases exponentially.

5 Practical implementations

The benefits of adopting new agile waveforms in 5G wireless communication systems has also been evaluated in the context of two practical FPGA-based implementations that reproduce two different coexistence scenarios that are envisioned to be highly relevant in 5G. After carefully considering the conclusions drawn in Sections 3 and 4 related to the coexistence of 5G waveforms with legacy ones in fragmented spectrum use cases and the associated computational complexity under fair comparison conditions, we have selected to implement a waveform based on the FBMC scheme. These real-time implementations allow to address the inherent digital design challenges of FBMC waveforms and also, in one of the cases, to experimentally validate the prime spectral efficiency and spectral characteristics of this 5G candidate waveform.

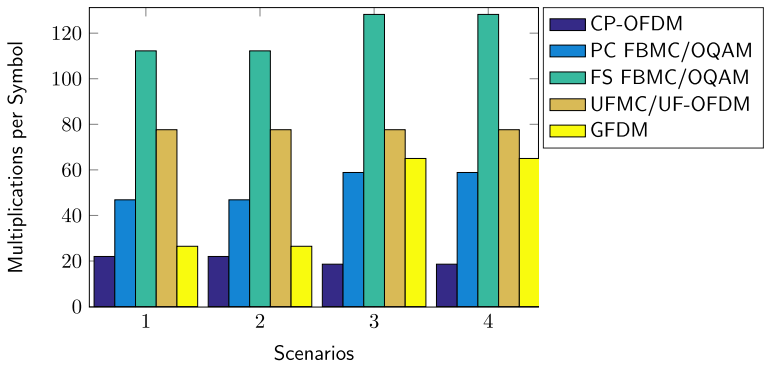

Fig. 10 Computational complexity in terms of number of real valued multiplications per Tx/Rx symbol in the base station

5.1 A flexible radio transceiver for TVWS based on FBMC

Dynamic spectrum sharing has been proposed to improve spectrum utilization. The digital switch over (DSO) in TV bands, which has resulted in making the so-called TV white space (TVWS) UHF spectrum available, was the first actual example where such a mechanism has been allowed. In 2009, the US radio regulator—the Federal Communication Commission (FCC)—authorized opportunistic unlicensed operation in the TV bands [27]. The initiative has recently been followed by the UK regulator (Ofcom) [28] and by the Ministry of Internal Affairs and Communications of Japan. In this context, opportunistic communication systems have to coexist with incumbent systems, i.e. TV broadcast signals. The coexistence scheme is enforced with a priority mechanism where opportunistic systems must guarantee that no harmful interference will be incurred to the incumbents. Harmful interference is defined in a twofold way. Firstly, co-channel communication between incumbent and opportunistic systems is prohibited. This means that opportunistic systems must be able to assess the presence of incumbent signals and access only channels vacant from any incumbent. Besides, opportunistic systems have a limited amount of time to evacuate the channel when an incumbent is switched on. Secondly, the adjacent channel leakage ratio (ACLR) is limited in order to prevent an opportunistic system from interfering with an incumbent operating in another channel, and in particular in adjacent channels. In [27], ACLR is restricted to be at least 55 dB. Such a high ACLR requirement is specific to the TVWS context and similar requirements are considered in other countries (e.g. in the UK [28]). These requirements of flexibility and stringent ACLR have led IEEE DYSPAN Standard Committee to identify the necessity to develop a new standard defining radio interface for white space radio systems: IEEE 1900.7 standard [29]. The standard is based on FBMC PHY. Through an implementation on a flexible hardware TVWS transmitter, [30] showed that FBMC modulation can meet ACLR levels prescribed by the FCCs coexistence requirements. The actual implementation was aimed at assessing the performance under real hardware impairment

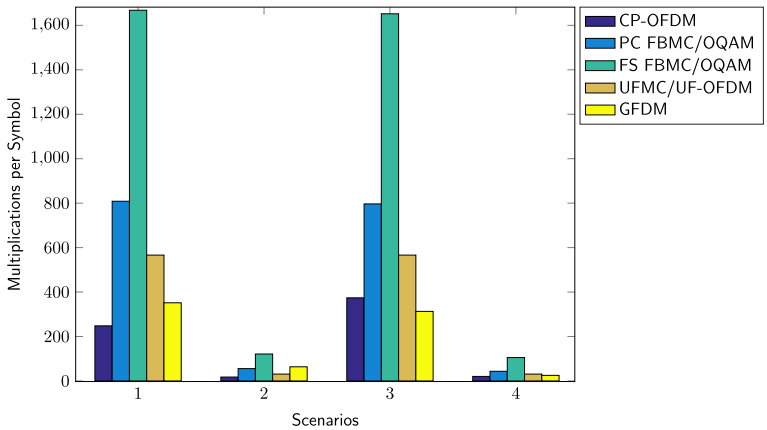

Fig. 11 Computational complexity in terms of number of real valued multiplications per Tx/Rx symbol in the base mobile station

conditions, such as limited dynamic range digital-to-analog converters (DAC). One of the main shortcomings of FBMC was supposed to be its implementation complexity. However, recent results have shown that a flexible approach was possible with very limited complexity overhead [30].

The complexity has been evaluated for a Xilinx Kintex-7 FPGA and is given by the amount of slice registers, look-up tables (LUT) and DSP48E1 cells used by the different modules of the receiver design. Slice registers correspond to the amount of register cells used, while LUT to the amount of combinatorial logic in the design. DSP48E1 cells are digital signal processing (DSP) cells dedicated to multiplication and accumulation (MAC) operations. The results have shown that the computational complexity of the FBMC transmitter is very similar to the OFDM transmitter complexity in this context. Furthermore, the receiver complexity is only around 30% higher than the one of the CP-OFDM receiver (see Table 2). In addition, the proposed block-wise processing approach requires FBMC symbols to be stored, which impacts the size of the memory (2.5x the one of an equivalent CP-OFDM RX). However, such memory sizes can be implemented at a very limited footprint and cost on current silicon technology nodes.

5.2 An agile FBMC waveform for fragmented spectrum use cases

In this section, we present the real-time FPGA implementation of an agile FBMC DL transmitter, designed to optimally exploit unused fragmented spectrum. The transmitter has been validated in a waveform cohabitation scenario that includes a real-life professional mobile radio (PMR) system operating in the 400 MHz band. The PMR terminals use the terrestrial trunked radio for police (TETRAPOL) air interface. The benefits of the FBMC waveform have been benchmarked versus an LTE system, and for this reason, the DL FBMC frame features high similarity with the LTE standard specifications (release 9). Each FBMC symbol comprises 72 active carriers with 15 kHz spacing within the 1.4-MHz signal bandwidth. This results in a 10-ms radio frame organized in ten subframes, containing 150 FBMC symbols. The first three symbols in each frame include a preamble which enables synchronization under non-contiguous spectrum. The pilot pattern is based on the reference signal structure of LTE with additional "auxiliary pilots" that compensate the contribution from surrounding symbols. The FBMC waveform uses a fast convolution scheme [31] with a short transform length of eight FFT bins per carrier spacing (i.e. 16 points) and a long transform length of 1024 points.

The DL FBMC and LTE transmitters feature a single- and a two-antenna configuration (i.e. based on the open-loop spatial multiplexing scheme of LTE) and they have been jointly implemented in an FPGA-based system-on-chip (SoC) device. The baseband design optimizes the utilization of processing resources in the different digital signal processing (DSP) stages. Time division multiplexing allows reusing only two 16-point FFT and two 1024-point IFFT engines to implement the MIMO FBMC scheme (i.e. 128 16-point FFTs are combined to provide the inputs to each large IFFT). The latter is based on an overlap and save convolution, which results in a variable number of samples in the input of each DSP stage and also a variable number of bits per sample for the fixed-point arithmetic operations. A latency-aware memory plane helps to minimize the embedded memory utilization and addresses the variable storage needs of the pipelined DSP architecture. Moreover, a centralized control unit has been designed to govern the synchronous communication of the diverse DSP stages. Finally, clock-gating techniques minimize the dynamic power consumption. Figure 12 shows the baseband design of the DL MIMO FBMC transmitter and Table 3 the overall implementation results in the target Xilinx XC7Z045 device.

The hardware setup described in [31] has been used to assess the TETRAPOL terminal performance when coexisting in the same band either with a MIMO FBMC or LTE transmission. A configurable spectral hole of 30 kHz has been left at the FBMC or LTE DL signal to accommodate

Table 2 Complexity comparison for FBMC implementation on Xilinx FGPA

	Complexity evaluation			
Architecture	Slice Regs	LUTs	DSP48E1	RAM BLKS
OFDM transmitter	10262	6752	14	14
FBMC transmitter	11300	7990	30	19
FBMC transmitter complexity overhead	10%	18%	114%	36%
OFDM receiver	42574	39600	97	49
FBMC receiver	54970	50096	155	171
FBMC receiver complexity overhead	29%	27%	60%	249%

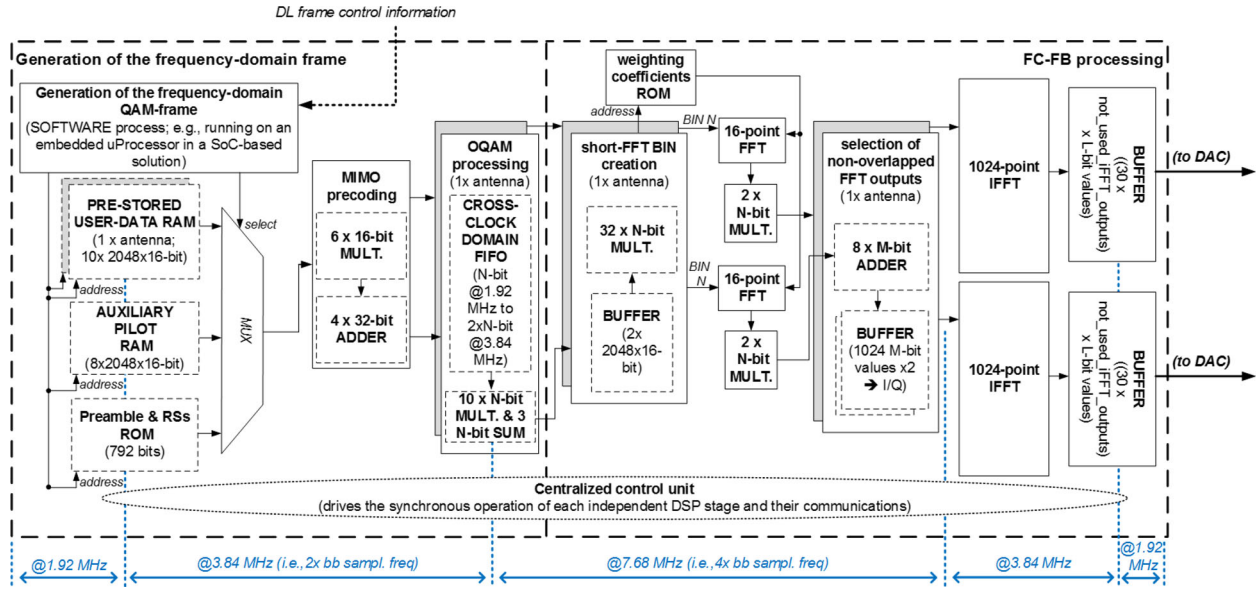

Fig. 12 Optimized digital baseband design of the MIMO FC-FBMC transmitter and detailed implementation metrics of the four different transmitters (SISO and MIMO, FC-FBMC and CP-OFDM) hosted in the FPGA-based SoC device

the 12.5 kHz TETRAPOL signal. The performance of the TETRAPOL terminal was evaluated by calculating the BER for different received signal powers and carrier power ratios between the coexisting signals, under an ITU vehicular-A mobile channel (50 km/h). Each curve shown in Fig. 13 averages 10.000 TETRAPOL frames for each measurement configuration. As it can be observed, the FBMC waveform offers superior interference protection to the coexisting TETRAPOL transmission (around 29 dB) when compared to LTE.

6 Conclusions

Flexible and efficient use of non-contiguous unused spectrum targeting heterogeneous mobile network deployment scenarios is one of the key challenges that future 5G systems would need to tackle. To maximize SE, the 5G air interface technologies will need to be flexible and capable of mapping various services to the best suitable combinations of frequency and radio resources. Alternatives to classic CP-OFDM have thus been intensively studied in the past few years. In this work, a fair comparison of several 5G multicarrier waveform candidates (OFDM, UFMC, FBMC, GFDM) has been conducted under a common framework. SE, power spectral density, PAPR and computational complexity have been assessed for the different waveforms. Resistance of the waveforms in a typical asynchronous multi-user uplink scenario, for different parametrisation and configuration, has also been addressed. A synthesis chart is depicted on Fig. 14. We have shown that UFMC waveform is an interesting option as the SE is comparable to that of OFDM and the pulse shaping function enhances the performance in the asynchronous multi-user scenario. UFMC also preserves backward compatibility with well-known OFDM algorithms (channel estimation, MIMO detectors). FBMC-OQAM and GFDM go a step further: interference between adjacent bands is minor, making these waveforms particularly interesting for 5G scenarios, at a price of slight complexity

Table 3 FPGA implementation metrics of the LTE and FBMC DL PHY-layer for the SISO and MIMO (open-loop spatial multiplexing) antenna schemes

System	Slices (%)	DSP48E1 (%)	RAMB18E1 (%)	RAMB36E1 (%)
SISO LTE	6	2	1	1
MIMO LTE	9	4	1	2
SISO FBMC	6	5	1	4
MIMO FBMC	13	11	2	10
ALL 4 TXs	26	18	4	16

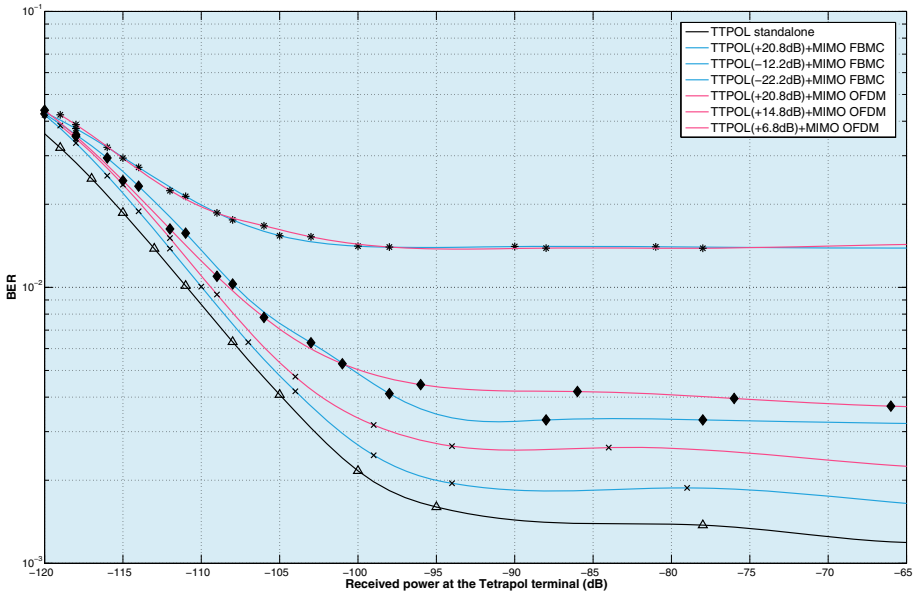

Fig. 13 Performance of the TETRAPOL terminal evaluated in relation to the interference received from the in-band MIMO broadband transmissions

increase. FBMC-OQAM is a promising solution even when it comes to practical implementations: in this paper, we have presented results that reveal the feasibility of the FBMC-OQAM waveform. We have demonstrated the relevance of FBMC especially when targeting the deployment of secondary systems in existing underutilized (and spectrally fragmented) bands, where interference protection of primary transmissions is mandatory. Two different DL FBMC systems were implemented and validated when coexisting at the same band either with primary PMR or TVWS transmissions. The efficient and non-interfering shared utilization of licensed spectrum (either between primary or primary and secondary transmissions) is a enabler of 5G systems [1] the benefits of which can also be applied on unlicensed shared spectrum access (or even combinations of the two).

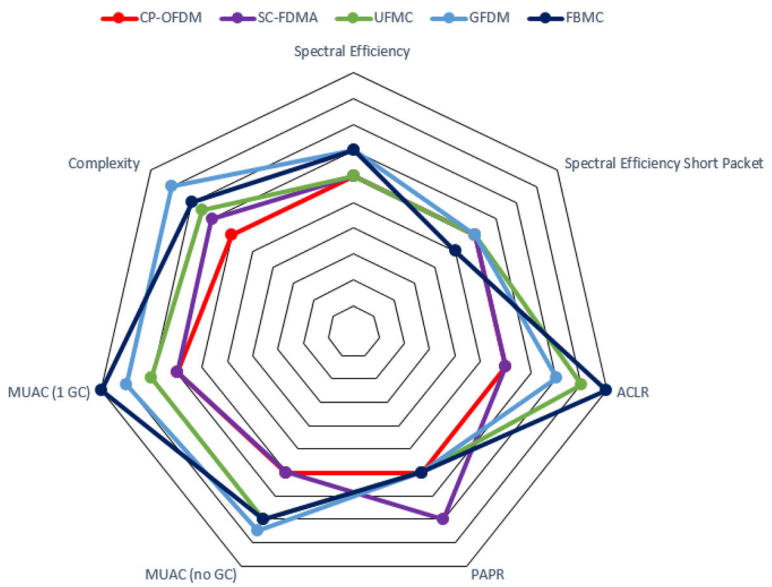

Fig. 14 Waveform comparison: synthesis

Acknowledgements
The work of Intel and CEA-Leti is partially supported by the European Commission under Horizon 2020 projects FANTASTIC-5G (GA 671660) and Flex5Gware (GA 671563). The work of CTTC was partially supported by the European Commission under the project EMPhAtiC (GA 318362) and currently partially supported by the Generalitat de Catalunya (2014 SGR 1551) and by the Spanish Government under project TEC2014-58341-C4-4-R.

Competing interests
The authors declare that they have no competing interests.

Author details
[1]CEA-Leti, Minatec Campus, Grenoble, France. [2]Centre Tecnológic de Telecomunicacions de Catalunya, Barcelona, Spain. [3]Intel Deutschland GmbH, Feldkirchen, Germany.

Received: 6 October 2016 Accepted: 12 December 2016
Published online: 11 January 2017

References

1. NGMN Alliance, Next Generation Mobile Networks Ltd, Frankfurt am Main (2015)
2. T Wild, F Schaich, Y Chen, in *19th International Conference on Digital Signal Processing (DSP)*. 5G air interface design based on universal filtered (UF-)OFDM, (2014), pp. 699–704. doi:10.1109/ICDSP.2014.6900754
3. F Zhao, Huawei smartphone solutions white paper (2012)
4. G Fettweis, M Krondorf, S Bittner, in *Proc. IEEE 69th Vehicular Technology Conference (VTC)*. GFDM—generalized frequency division multiplexing, (2009), pp. 1–4. doi:10.1109/VETECS.2009.5073571
5. M Bellanger, in *5th International Symposium on Communications Control and Signal Processing (ISCCSP)*. FS-FBMC: an alternative scheme for filter bank based multicarrier transmission, (2012), pp. 1–4. doi:10.1109/ISCCSP.2012.6217776
6. N Michailow, I Gaspar, S Krone, M Lentmaier, G Fettweis, in *International Symposium on Wireless Communication Systems (ISWCS)*. Generalized frequency division multiplexing: analysis of an alternative multi-carrier technique for next generation cellular systems, (2012), pp. 171–175. doi:10.1109/ISWCS.2012.6328352
7. A Sahin, I Guvenc, H Arslana, A survey on multicarrier communications: prototype filters, lattice structures, and implementation aspects. IEEE Commun. Surv. Tutor. **16**(3), 1312–1338 (2014)
8. F Schaich, T Wild, in *6th International Symposium on Communications, Control and Signal Processing (ISCCSP)*. Waveform contenders for 5G 2014; OFDM vs. FBMC vs. UFMC, (2014), pp. 457–460. doi:10.1109/ISCCSP.2014.6877912
9. AA Zaidi, J Luo, R Gerzaguet, A Wolfgang, RJ Weiler, J Vihriala, T Svensson, Y Qi, H Halbauer, Z Zhao, P Zetterberg, H Miao, in *Proc. IEEE 83rd Vehicular Technology Conference (VTC Spring)*. A preliminary study on waveform candidates for 5G mobile radio communications above 6 GHz, (2016), pp. 1–6. doi:10.1109/VTCSpring.2016.7504096
10. J Nadal, CA Nour, A Baghdadi, H Lin, in *Proc. 25th IEEE International Symposium on Rapid System Prototyping (RSP)*. Hardware prototyping of FBMC/OQAM baseband for 5G mobile communication, (2014), pp. 72–77. https://hal.archives-ouvertes.fr/hal-01170367
11. P Weitkemper, J Koppenborg, J Bazzi, R Rheinschmitt, K Kusume, D Samardzija, R Fuchs, A Benjebbour, in *Proc. IEEE Wireless Communications and Networking Conference (IWCNC)*. Hardware experiments on multi-carrier waveforms for 5G, (2016), pp. 1–6. doi:10.1109/WCNC.2016.7564682
12. F Kaltenberger, R Knopp, C Vitiello, M Danneberg, A Festag, in *Proc. the Joint NEWCOM/COST Workshop on Wireless Communications (JNCW)*. Experimental Analysis of 5G Candidate Waveforms and their Coexistence with 4G Systems, (2015). http://www.eurecom.fr/fr/publication/4725/download/cm-publi-4725.pdf
13. D Garcia-Roger, JF de Valgas, N Incardona, JF Monserrat, C Narcis, in *Proc. IEEE International Symposium on Personal, Indoor and Mobile Radio Communications (PIMRC)*. Hardware testbed for sidelink transmission of 5G waveforms without synchronization, (2016)
14. G Jue, Flexible Testbed for 5G Waveform Generation and Analysis. Microw. J, 12–14 (2015)
15. Rohde & Schwarz, 5G Waveform Candidates. Application Note 1MA271 (2016)
16. M Bellanger, in *IEEE Radio and Wireless Symposium (RWS)*. Physical layer for future broadband radio systems, (2010), pp. 436–439. doi:10.1109/RWS.2010.5434093
17. DS Waldhauser, LG Baltar, JA Nossek, in *Proc. IEEE 9th Workshop on Signal Processing Advances in Wireless Communications*. MMSE subcarrier equalization for filter bank based multicarrier systems, (2008), pp. 525–529. doi:10.1109/SPAWC.2008.4641663
18. J-B Dore, V Berg, N Cassiau, D Ktenas, FBMC receiver for multi-user asynchronous transmission on fragmented spectrum. EURASIP J. Adv. Signal Process. **2014**(1), 41 (2014)
19. R Datta, N Michailow, M Lentmaier, G Fettweis, in *Proc. IEEE Vehicular Technology Conference (VTC Fall)*. GFDM interference cancellation for flexible cognitive radio PHY design, (2012), pp. 1–5. doi:10.1109/VTCFall.2012.6399031
20. I Gaspar, M Matthé, N Michailow, LL Mendes, D Zhang, G Fettweis, Frequency-Shift Offset-QAM for GFDM. IEEE Communications Letters. **19**(8), 1454–1457 (2015)
21. G Wunder, P Jung, M Kasparick, T Wild, F Schaich, Y Chen, S Brink, I Gaspar, N Michailow, A Festag, L Mendes, N Cassiau, D Ktenas, M Dryjanski, S Pietrzyk, B Eged, P Vago, F Wiedmann, 5GNOW: non-orthogonal, asynchronous waveforms for future mobile applications. Commun. Mag. IEEE. **52**(2), 97–105 (2014)
22. LG Baltar, F Schaich, M Renfors, JA Nossek, in *2011 Future Network Mobile Summit*. Computational complexity analysis of advanced physical layers based on multicarrier modulation, (2011), pp. 1–8
23. M Bellanger. FBMC physical layer: a primer, (2010). http://www.ict-phydyas.org
24. T Wild, F Schaich, in *2015 IEEE 81st Vehicular Technology Conference (VTC Spring)*. A Reduced Complexity Transmitter for UF-OFDM, (2015), pp. 1–6
25. Y Chen, F Schaich, T Wild, in *2014 IEEE 79th Vehicular Technology Conference (VTC Spring)*. Multiple Access and Waveforms for 5G: IDMA and Universal Filtered Multi-Carrier, (2014), pp. 1–5. doi:10.1109/VTCSpring.2014.7022995
26. I Gaspar, N Michailow, A Navarro, E Ohlmer, S Krone, G Fettweis, in *2013 IEEE 77th Vehicular Technology Conference (VTC Spring)*. Low Complexity GFDM Receiver Based on Sparse Frequency Domain Processing, (2013), pp. 1–6. doi:10.1109/VTCSpring.2013.6692619
27. FCC Final Rule: Unlicenced operation in the TV broadcast bands. US Fed. Regist. **74**(30), 7314–7332 (2009)
28. Ofcom, Implementing TV white spaces (2015)
29. IEEE P1900.7 PAR, Radio interface for white space dynamic spectrum access radio systems supporting fixed and mobile operation (2011)
30. V Berg, J-B Dore, D Noguet, in *9th International Conference on Cognitive Radio Oriented Wireless Networks and Communications (CROWNCOM), 2014*. A flexible FS-FBMC receiver for dynamic access in the TVWS, (2014), pp. 285–290. doi:10.4108/icst.crowncom.2014.255866Z
31. O Font-Bach, N Bartzoudis, X Mestre, D Lopez-Bueno, P Mege, L Martinod, V Ringset, TA Myrvoll, When SDR meets a 5G candidate waveform : agile use of fragmented spectrum and interference protection in PMR networks. IEEE Wirel. Commun. **22**(6), 56–66 (2015)